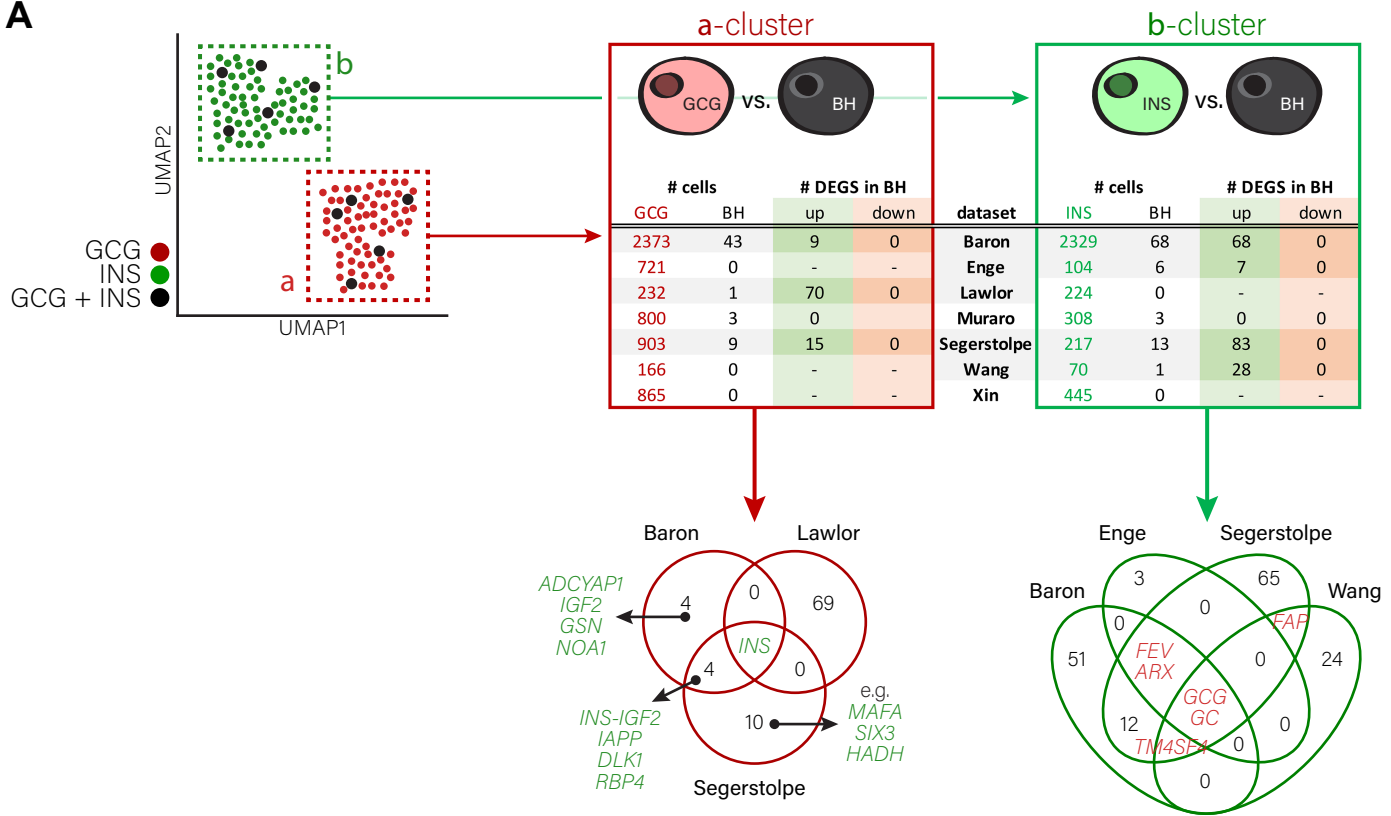
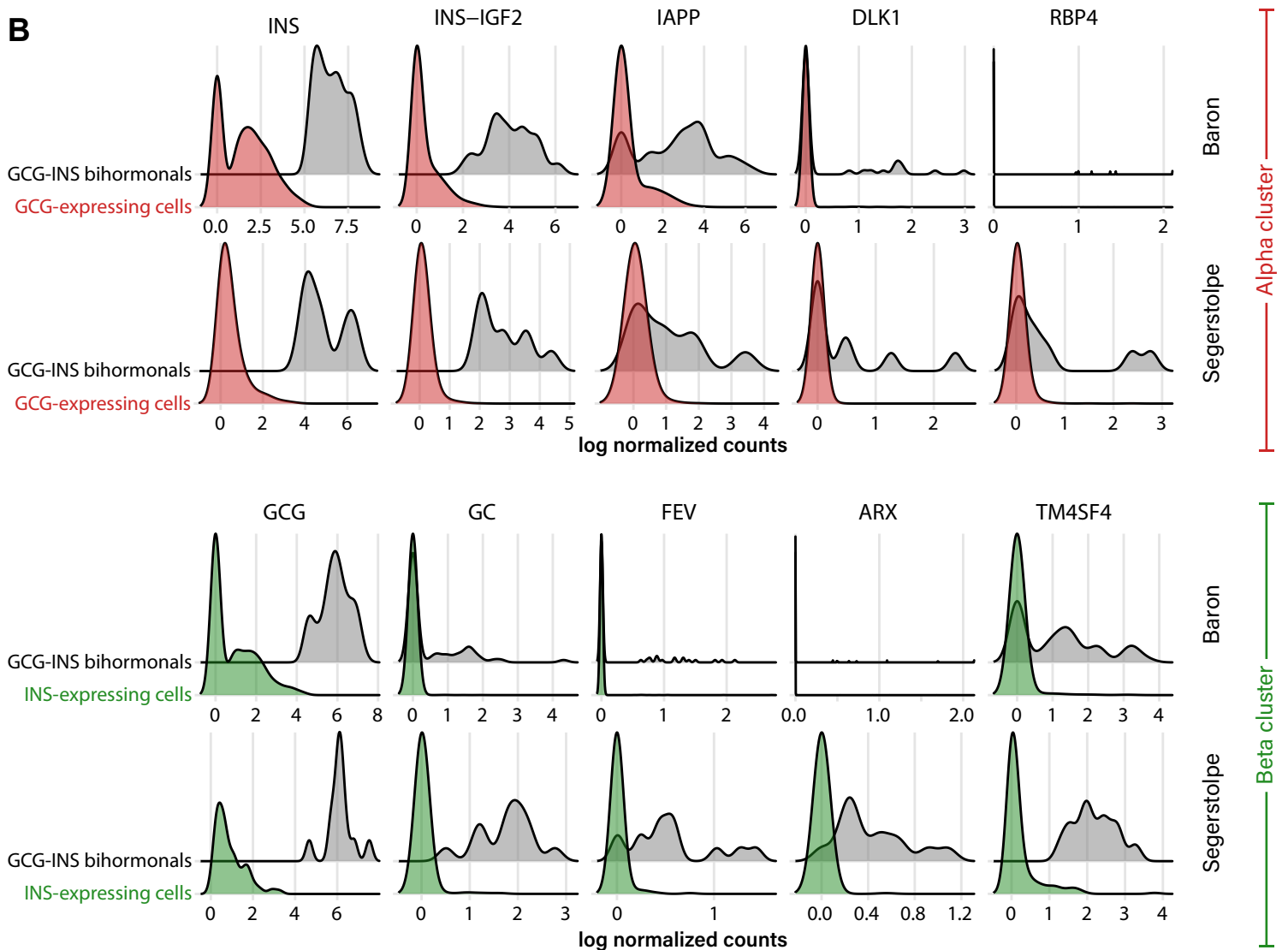
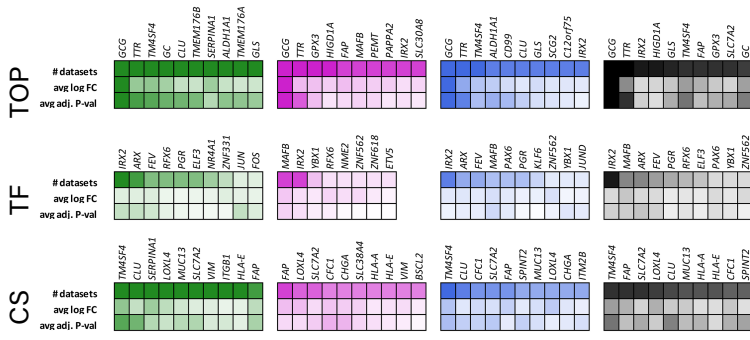
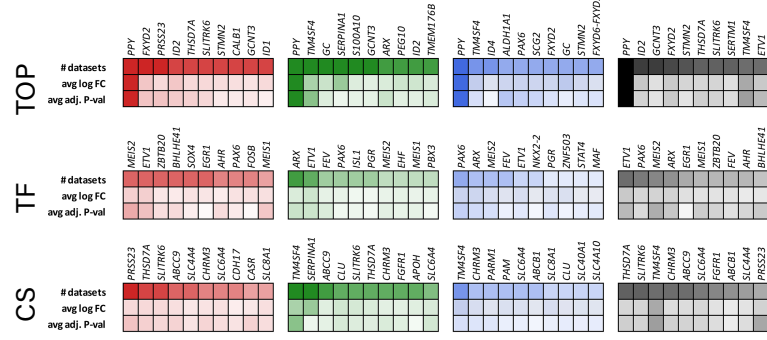
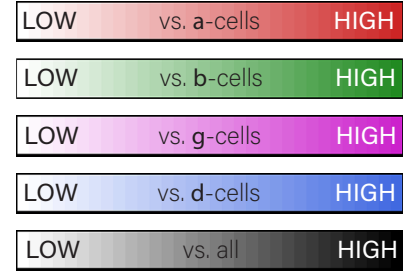
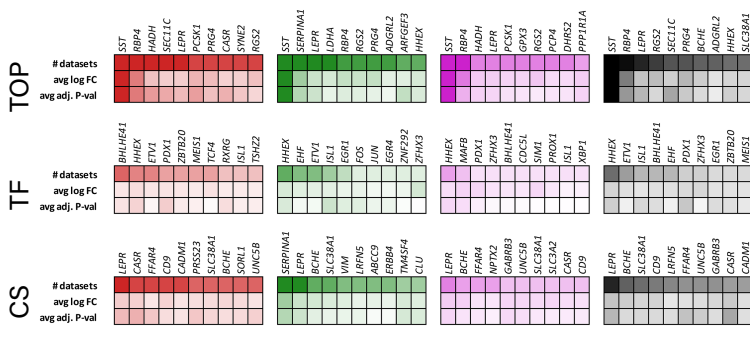
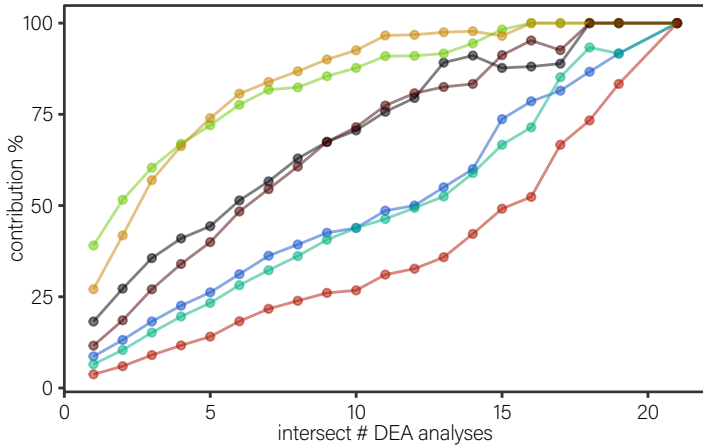
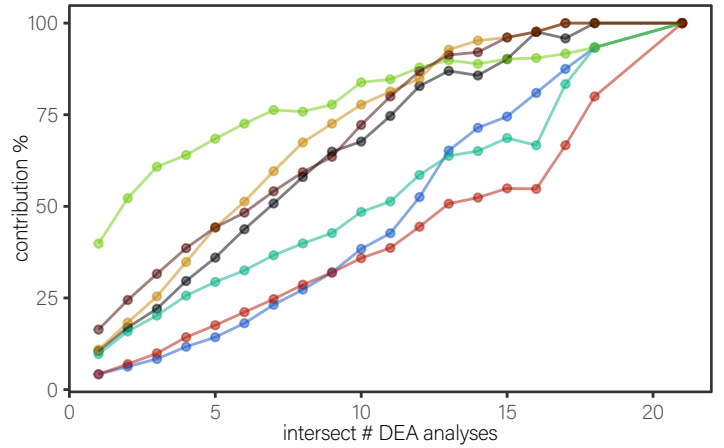
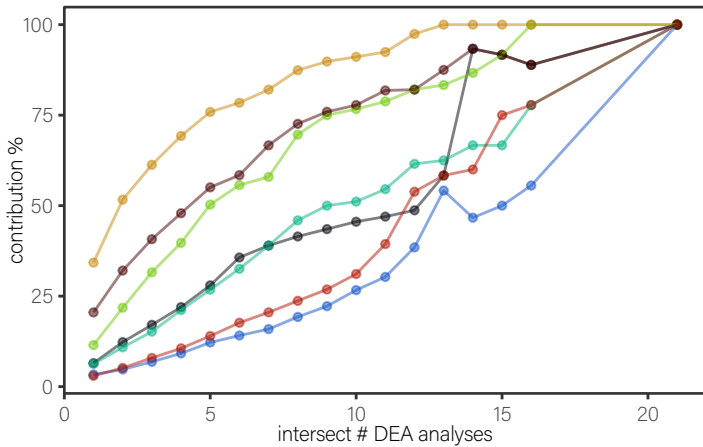
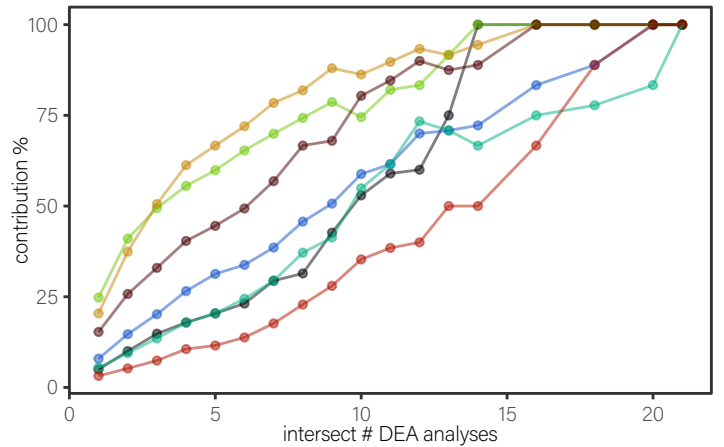


Supplemental figure 1. Generation and filtering of individual single-cell transcriptomics datasets. A) UMAP dimension reduction plots of individual datasets after processing and filtering, indicated per dataset of each author. B) Examples of identification of doublets within datasets. Cells are color-coded based on which tool was used to identify them as doublets. The black arrow in the Muraro dataset indicates an area with a high concentration of cells that were indicated as doublets by both Scrublet and DoubletFinder. C) After final cell type allocation, endocrine cell type abundance was assessed for both NDM and T2DM cells, per dataset. There were no significant differences in abundance between NDM and T2DM cell types. D) Percentage of bi-hormonal cells, relative to its mono-hormonal counterparts. For example, the percentage of GCG-INS bi-hormonal cells is calculated over the total number of monohormonal cells that express either GCG or INS. Values were calculated per dataset in both non-diabetic (NDM) and type 2 diabetic (T2DM) populations, when applicable. Red lines connect NDM and T2DM data from the same dataset.

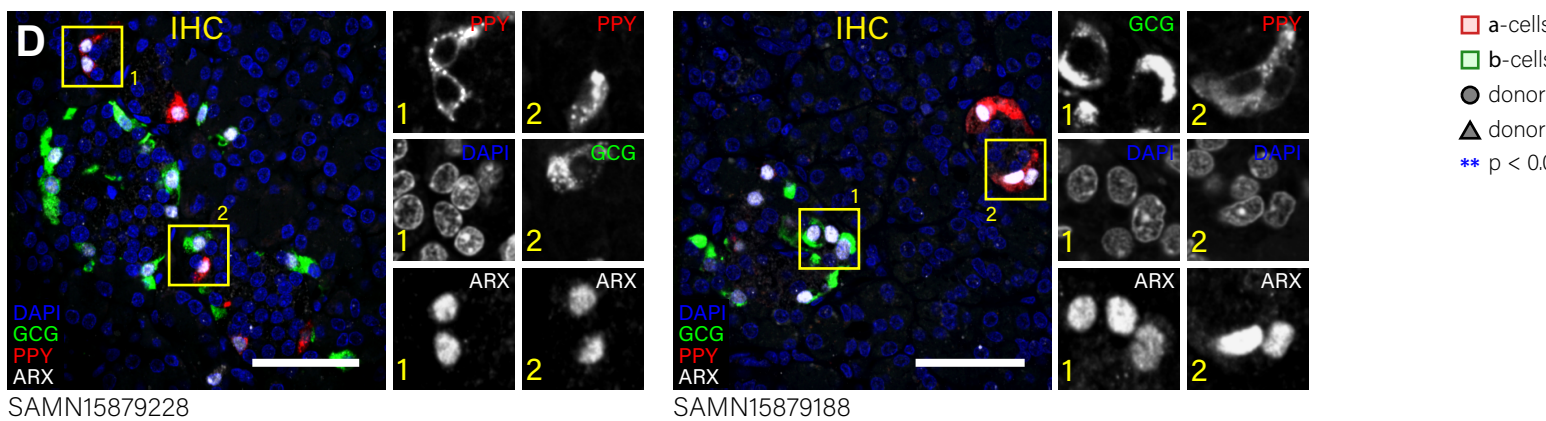
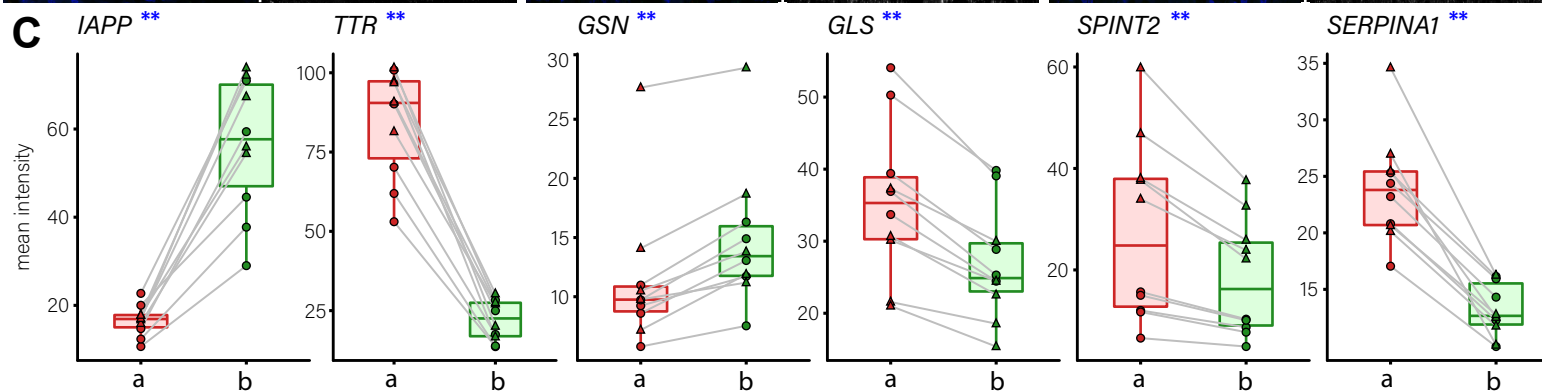
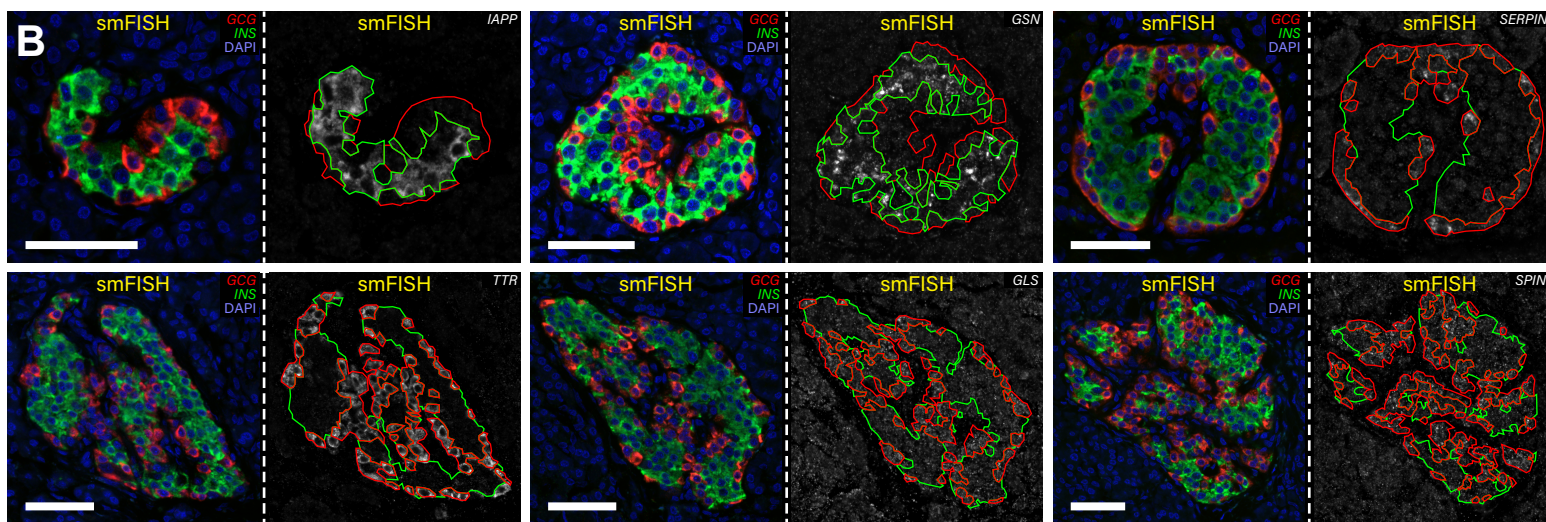
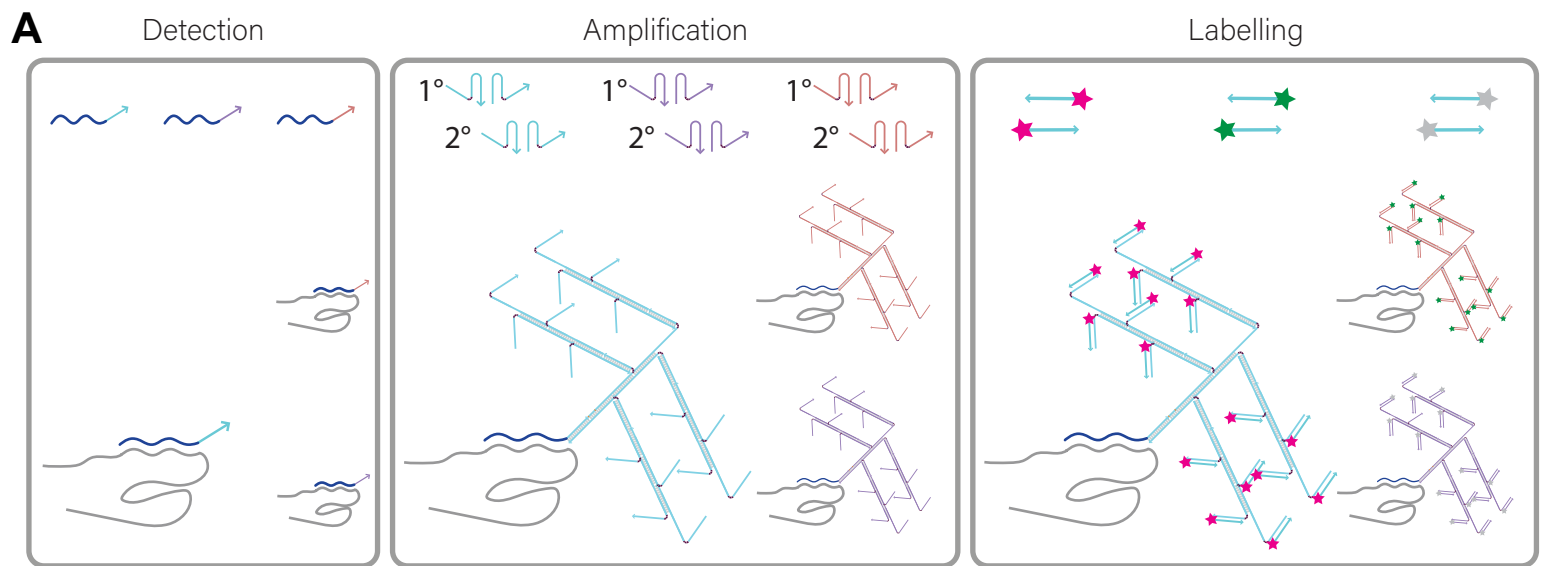
A**B**

Supplemental figure 2. Profiling of bihormonal cells. A) Characterization of bi-hormonal cells within α - and β -cell clusters. Within each cluster, differentially expressed genes were calculated between bi-hormonal cells and their mono-hormonal counterparts, as indicated in the table. Upregulated but no downregulated genes were found in the bi-hormonal cells. Per cell type cluster, upregulated genes were intersected to visualize genes that were upregulated in bihormonal cells in more than one dataset. B) Ridge plots depicting log normalized expression distribution in bihormonal cells vs. GCG expressing cells in the α -cell cluster, and vs. INS expressing cells in the β -cell cluster, in the Baron and Segerstolpe datasets.

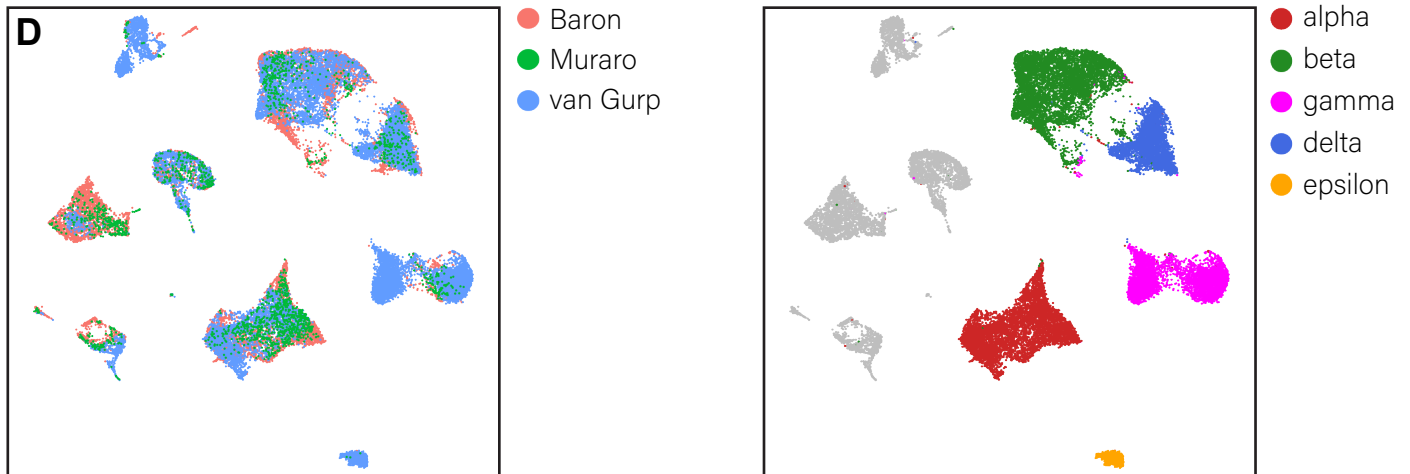
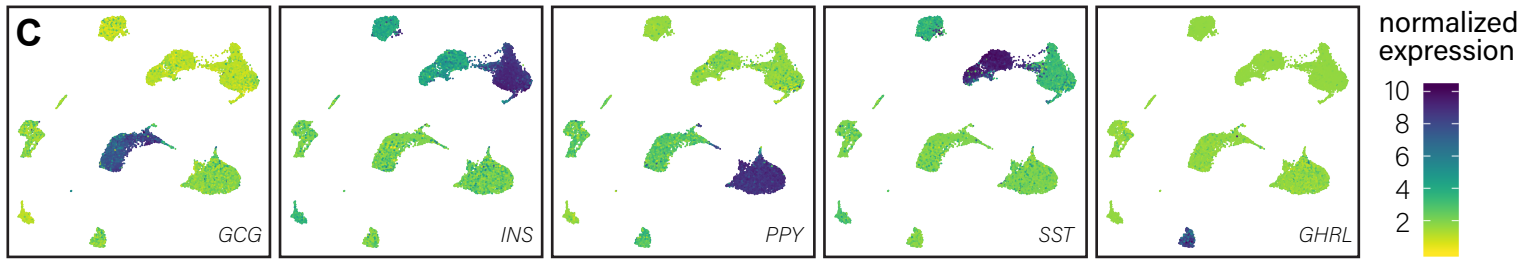
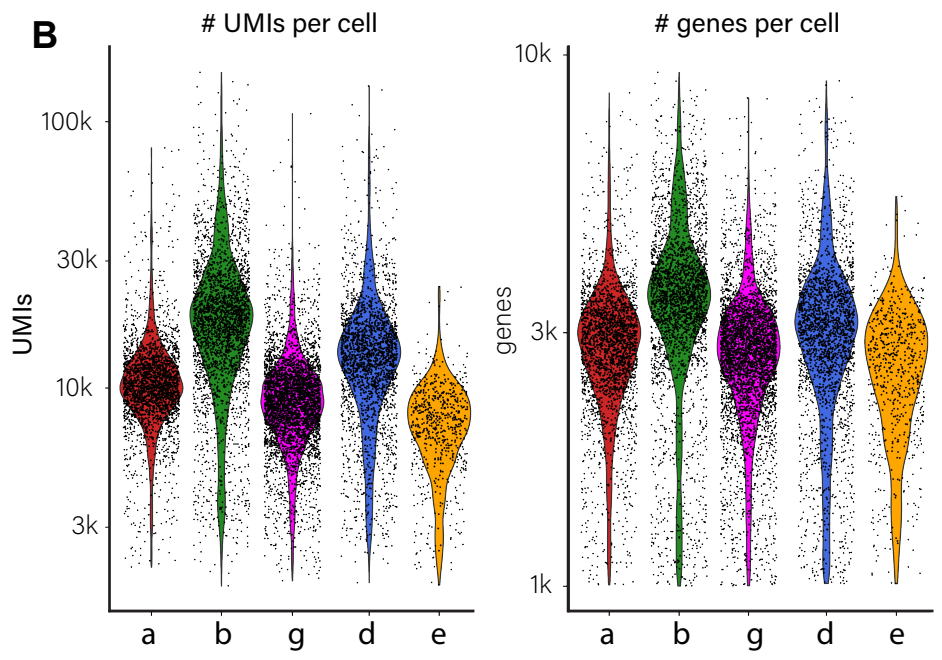
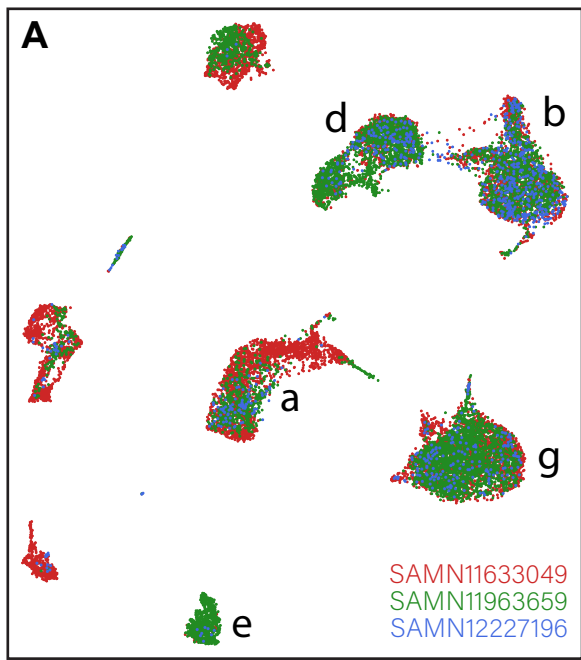
A**Alpha cell ID genes****Gamma cell ID genes****Delta cell ID genes****B****Alpha cell ID genes****Beta cell ID genes****Gamma cell ID genes****Delta cell ID genes**

— baron — engle — lawlor — muraro — segerstolpe — wang — xin

Supplemental figure 3. Defining identity genes for the different islet cell types. A) Top differentially expressed genes (TOP), top transcription factors (TF) and top genes that encode cell-surface proteins (CS) that characterize α -, γ - and δ -cells, in direct comparisons (vs. α -cells in red, vs. β -cells in green, vs. γ -cells in magenta and vs. δ -cells in blue, respectively), and in a combined manner to define general identity genes (in black). Genes were order primarily on the # analyses in which they were found to be differentially expressed, then based on a rank score that comprised both the adjusted p-value and the log fold-change. Darker colors indicate a higher number of analyses, a higher log fold-change or a more significant adjusted p-value. B) Per cell type, the contribution of individual datasets to the total number of genes that are retrieved in at least the intersected number of analyses on the X-axis.



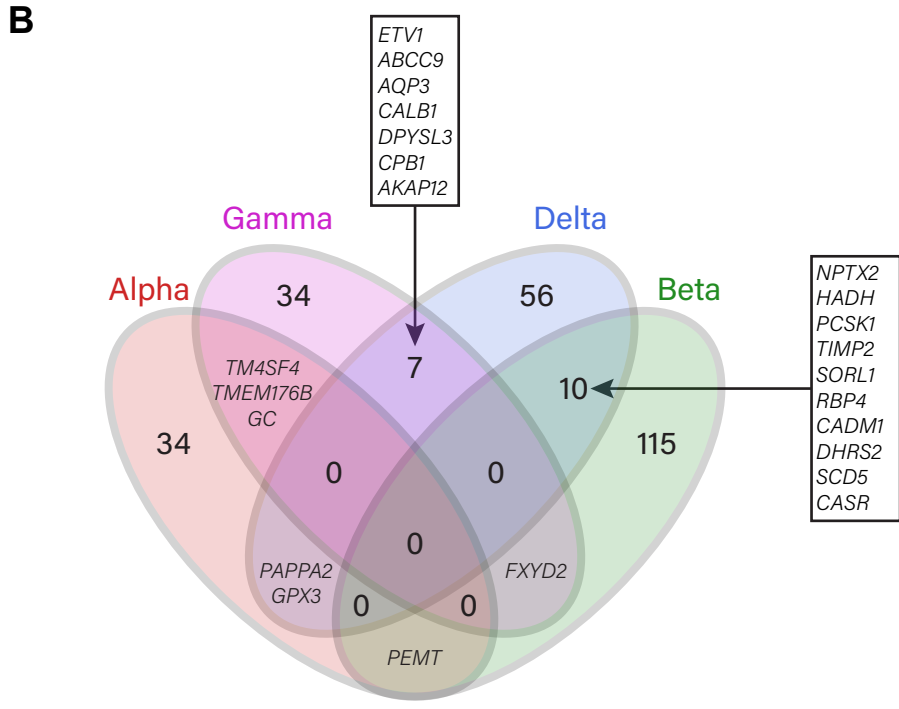
Supplemental figure 4. Orthologous validation of α - and β -cell identity markers. A) methodology for MUSE-based multiplex smFISH. Between 9 and 22 probes were annealed per mRNA target. During the primary and secondary reactions, hairpin DNA structures unfold to build an amplification tree. During labelling, fluorescent dyes were coupled to these trees to amplify the signal of each bound mRNA probe. B) Representative images for each measured probe in human FFPE pancreatic tissue. Per probe, two images are provided: a composite smFISH image for *INS* and *GCG* with DAPI (left), and the monochromatic image of the gene of interest, with outlines for α - and β -cells derived from the *GCG* and *INS* signals, respectively (right). C) Measured mean intensities in paired α - and β -cells from the same islet (2 donors, 5 islets per donor). Boxplot for α -cells in red, for β -cells in green. Paired data connected via grey line. Donor 1 in circles, donor 2 in triangles. Statistical analysis performed as Wilcoxon signed rank test, ** = $p < 0.01$. D) Representative images of ARX staining in both α - and γ -cells, in 2 independent donors (RRID: SAMN15879228 and SAMN15879188). Outlines illustrate specificity to α - and γ -cells, and overlap with DAPI.



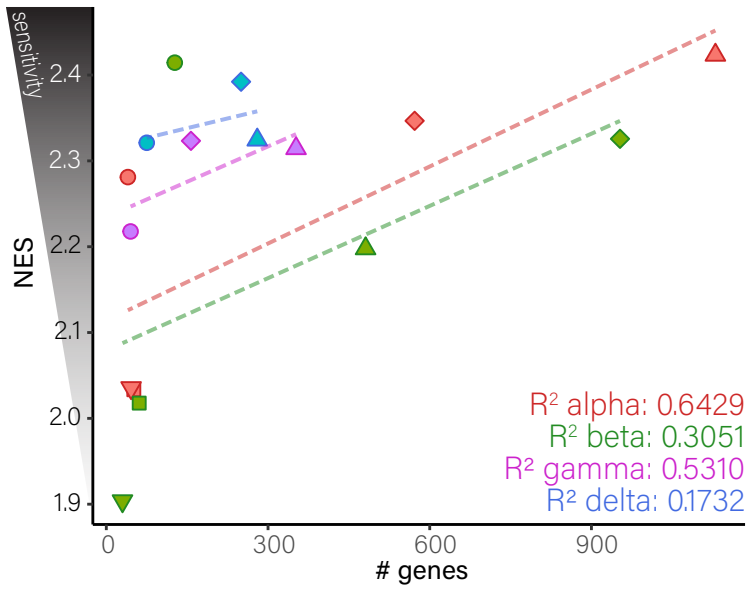
Supplemental figure 5. Quality assessment of our novel γ -, δ - and ε -cell enriched dataset.

A) Overlap of cells originating from different independent donors (RRID: SAMN11633049, SAMN11963659 and SAMN12227196). Cells are color-coded based on the donor they originate from. Cluster identities for endocrine cells are indicated by Greek letters. B) Data complexity of the novel dataset. For each cell type, the number of UMIs and genes per cell is indicated. C) UMAP dimensional reduction plots of the novel dataset, where cells are color-coded based on normalized hormone expression. D) Merged UMAPs of Baron, Muraro and our novel γ - δ - and ε -cell enriched datasets, color coded by either dataset origin or cell type.

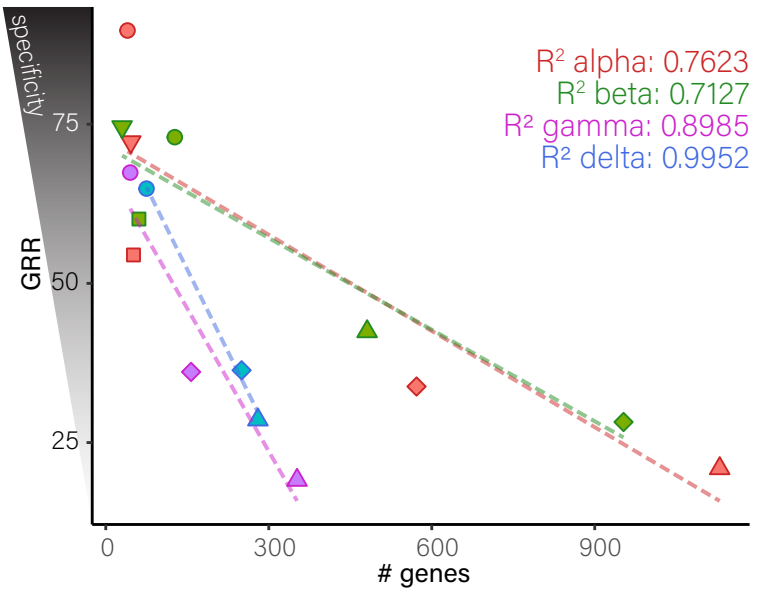
A α-ID (IS# 13) 40 genes	β-ID (IS# 8) 127 genes			γ-ID (IS# 8) 45 genes	δ-ID (IS# 6) 75 genes	
ALDH1A1	ABCC8	KCNK16	RPL4	ABCB1	ABCC9	NLRP1
B2M	AC099548.2	LDHB	RPL5	ABCC9	ABI3BP	NPTX2
CFC1	ADCYAP1	MAFA	RPL7	AKAP12	ADGRL2	OPRD1
CLU	ALCAM	MAFB	RPL7A	AMOTL1	AKAP12	PAPPA2
CRYBA2	ALDOA	MAP1B	RPS23	AQP3	AMIGO2	PCP4
CYSTM1	ARG2	MT-CO1	RPS3	ARX	ANK1	PCSK1
DPP4	ARL6IP5	MT-CO3	RPS4X	C16orf45	AQP3	PDLIM4
F10	ATP2A3	MT-CYB	RPS6	CALB1	ARFGEF3	PKIB
FAP	C1orf127	MT-ND1	RRAGD	CARTPT	BAIAP3	PLEKHB1
FXYD3	C1QL1	MT-ND2	SAMD11	CHN2	BCHE	PRG4
FXYD5	CADM1	MT-ND3	SCD	CHRM3	BHLHE41	PSIP1
GC	CASR	MT-ND4	SCD5	CPB1	C22orf42	RASSF6
GCG	CDKN1A	MTRNR2L1	SCG3	DPYSL3	CADM1	RBP4
GLS	CDKN1C	MTRNR2L10	SCGN	ETV1	CALB1	RGS2
GPX3	CNP	MTRNR2L12	SELENOW	FGFR1	CASR	S100A6
HIGD1A	CYP2U1	MTRNR2L6	SERINC1	FXYD2	CBLN4	SCD5
HLA-A	CYYR1	MTRNR2L8	SLC30A8	FXYD6-FXYD2	CD9	SEC11C
HLA-E	DBI	MTUS2	SLC39A14	GC	CPB1	SERPINA1
IRX2	DHRS2	MXRA7	SLC6A6	GCNT3	CXADR	SLC17A6
ITGB1	DHRS7	NECTIN3	SORL1	ID1	DHRS2	SLC38A1
KCTD12	DLK1	NKX6-1	STX1A	ID2	DIRAS3	SORL1
LOXL4	DNAJB9	NPTX2	SURF4	ID4	DPYSL3	SST
MUC13	EIF4A2	P2RY1	SUSD4	INPP5F	EDN3	SYNE2
NAA20	ELMO1	PAPSS2	SYT13	MEIS2	EHF	TENM3
PALLD	ENO1	PCSK1	TGFBR3	PAX6	ERBB4	TIMP2
PAPPA2	ENTPD3	PDX1	TIMP2	PEG10	ETV1	TMSB4X
PCSK2	ERO1B	PEBP1	TMEM150C	PPY	EYS	TPPP3
PEMT	FAM105A	PEMT	TMEM37	PTP4A3	F5	UNC5B
PLCE1	FAM159B	PERP	TNS1	PXK	FAM102A	VIM
PLIN3	FXYD2	PFKFB2	TPM3	S100A10	FFAR4	VMP1
RGS4	G3BP1	PFN2	TSPAN1	SCG2	FRZB	
RNASEK	G6PC2	PHACTR2	TSPAN13	SCGB2A1	GABRB3	
SLC7A2	GAD2	PLCXD3	UCHL1	SEMA3E	GPX3	
SMIM24	GLIS3	PPP1R1A	VEGFA	SERTM1	HADH	
SPINT2	GNAS	PRDX1	WARS	SLC4A4	HHEX	
TM4SF4	GSN	PRUNE2	WSCD2	SLC6A4	ISL1	
TMEM176A	HADH	PSAP	YWHAQ	SLITRK6	LDHA	
TMEM176B	HERPUD1	PTEN		SPINK1	LEPR	
TTR	HSP90AB1	RBP4		SPOCK1	LRFN5	
VGF	HSPA8	RGS16		STMN2	MDK	
	IAPP	ROBO2		THSD7A	MLPH	
	IGF2	RPL17		TM4SF4	MS4A8	
	INS	RPL23		TMEM176B	MTUS1	
	INS-IGF2	RPL24		TMEM47	NCOA7	
	ITPR3	RPL3		TXNIP	NDRG4	



Supplemental figure 6. Composition and overlap of the novel identity genesets. A) Composition of the four identity genesets, α -ID, β -ID, γ -ID and δ -ID. B) Venn diagram showing genes overlapping between identity genesets.

A Normalized enrichment vs. # genes per geneset

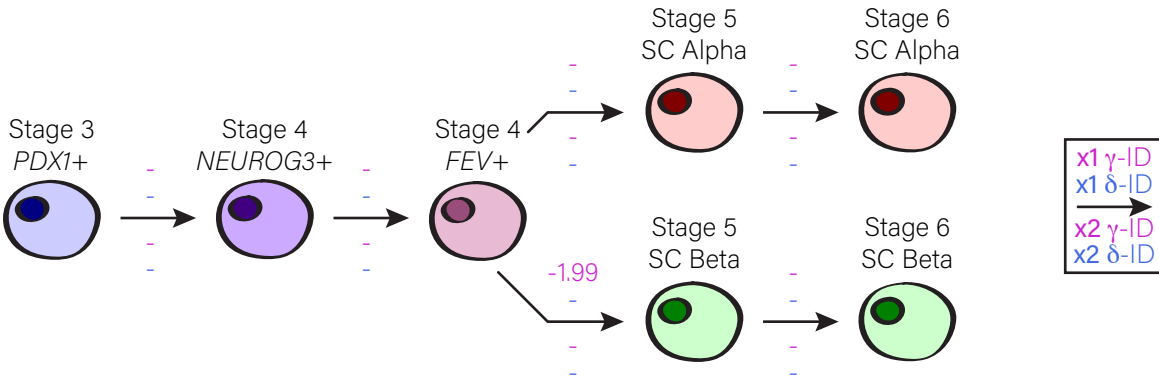
ID genesets ●
 Lawlor ■
 Muraro ◆
 Segerstolpe ▲
 Xin ▼

B Gene retrieval vs. # genes per geneset

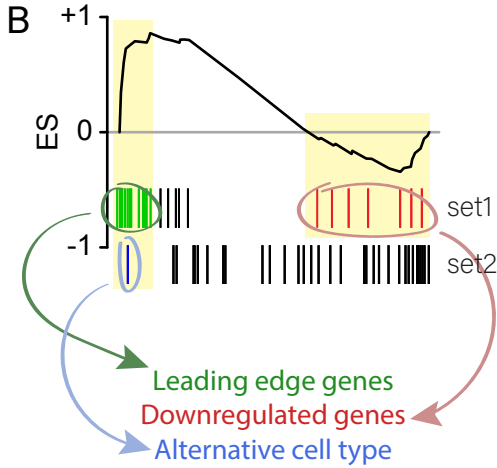
Alpha
 Beta
 Gamma
 Delta

Supplemental figure 7. Relationships between the number of genes, normalized enrichment scores and gene retrieval rates in genesets. A) The relationship between the number of genes in a dataset and the normalized enrichment score indicates a higher NES for genesets with more genes. Trendlines are color coded per cell type. B) The relationship between the number of genes in a dataset and the gene retrieval rate indicates a lower GRR for genesets with more genes. Trendlines are color coded per cell type. Shapes of individual points indicate the dataset of origin, while color indicates the associated cell type.

A

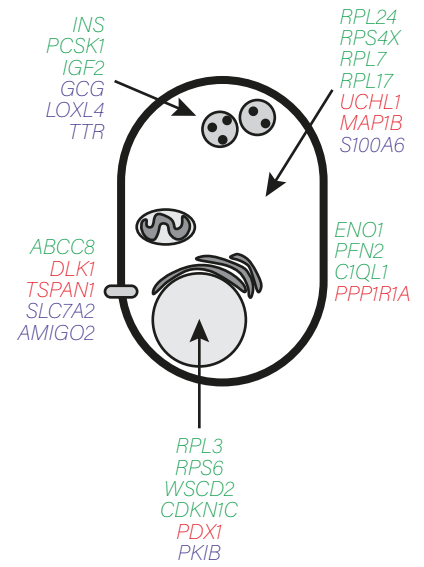
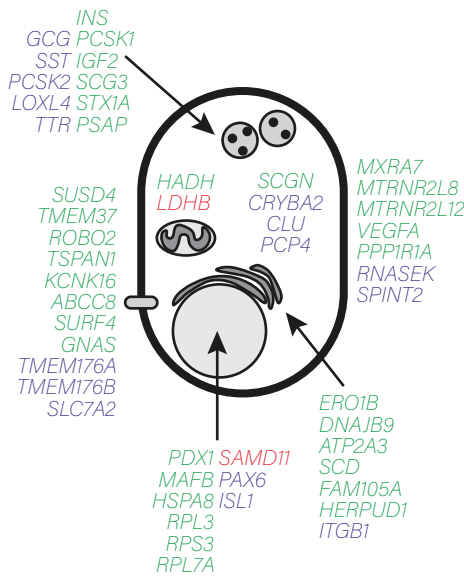


x1 protocol



C: s4 FEV → s5 SC-Beta

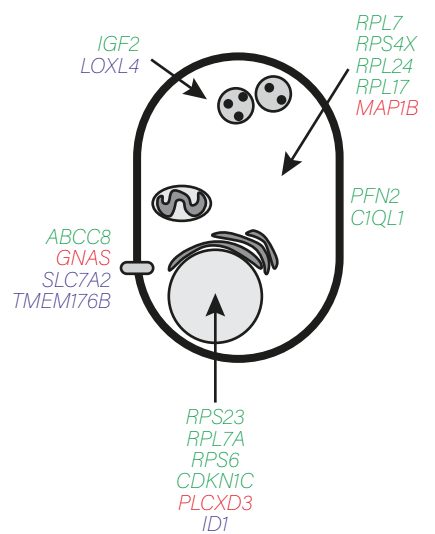
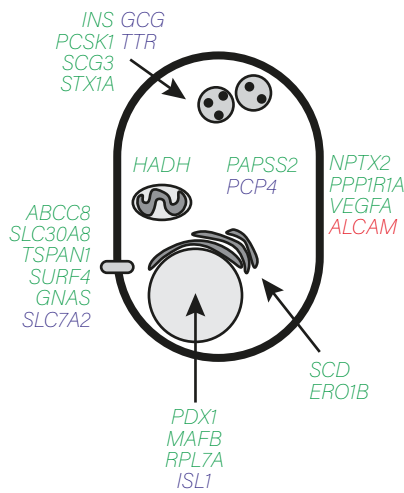
D: s5 SC-Beta → s6 SC-Beta



x2 protocol

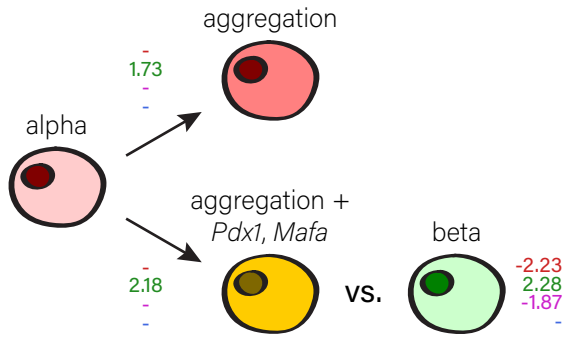
E: s4 FEV → s5 SC-Beta

F: s5 SC-Beta → s6 SC-Beta

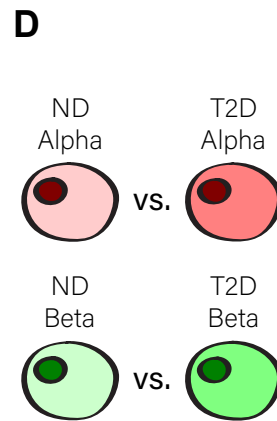
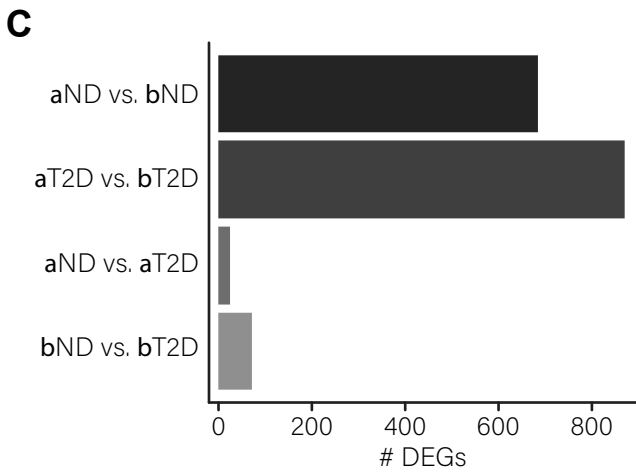
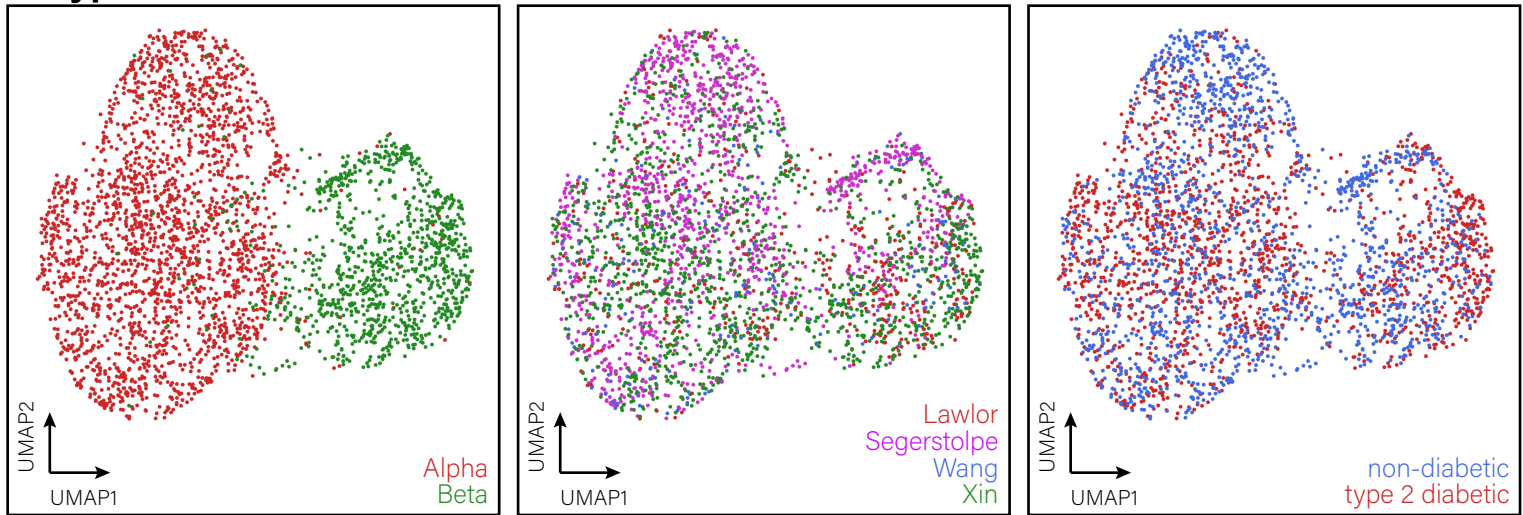


Supplemental figure 8. Deep profiling of SC- β cell identity changes. A) Changes in gamma and delta cell identity in different human ES/iPS differentiation protocols. B) Definition of different categories of genes. Leading edge genes are the gene that are responsible for the initial push during GSEA, and are thus the genes responsible for the observed correlation between geneset and phenotype. Downregulated genes are genes that have negative rank scores that are thus responsible for a pull towards the alternative phenotype. Alternative cell type genes are genes that are observed in genesets for the other islet cell types, that are regulated within the leading-edge region of the GSEA. These genes regulate an acquisition of phenotypical changes related to another cell type than the one intended. C-F) Summary cartoons depicting leading edge, downregulated and alternative cell type genes for progression from stage 4 FEV expressing progenitors to stage 5 SC- β cells (C, E), and from stage 5 to stage 6 SC- β cells (D, F) in both the x1 (C, D) and x2 (E, F) differentiation protocols. Leading edge genes in green, downregulated genes in red and alternative cell type genes in blue.

A: adult conversion



B: type 2 diabetes



Supplemental figure 9. Additional assessment of identity regulation during adult cell type conversion and between non-diabetic and type 2 diabetic islet cells. A) Changes in α -, β -, γ - and δ -cell identity were measured between states during adult cell type conversion. Values in red, green, magenta and blue indicate normalized enrichment scores from GSEA for α -ID, β -ID, γ -ID and δ -ID genesets, where positive values indicate a gain in identity and negative values indicate a loss of identity; ns = not significant (FDR 0.05 or higher). B) UMAP dimensional reduction of the combined dataset containing α - and β -cells from the Lawlor, Segerstolpe, Wang and Xin datasets. Color codes indicate either cell type (left), dataset origin (middle) or diabetes status (right). C) The total number of differentially expressed genes between non-diabetic (ND) α - and β -cells, type 2 diabetic (T2D) α - and β - cells, ND and T2D α -cells and ND and T2D β -cells in the combined dataset. D) Changes in α -, β -, γ - and δ -cell identity were measured between ND and T2D α - and β -cells. No changes were found in any identity geneset.

Dataset		Donors		Library preparation		Median reads/cell	Thresholds			Specific parameters	
First author	Last author	NDM	T2DM	Isolation	Processing		# counts	# genes	% mito	# var genes	# sig PCs
Baron	Yanai	3	1	inDrop	CEL-seq	100k	UMIs 800	200	20	765	40
Enge	Quake	5	-	FACS	SMARTseq2	950k	100'000	2'500	15	832	16
Lawlor	Stitzel	5	3	Fluidigm C1	SMARTseq	3'000k	450'000	5'000	20	1'153	10
Muraro	van Oudenaarden	4	-	FACS	CEL-seq2	90k	UMIs 2'000	350	25	1'069	40
Segerstolpe	Sandberg	6	4	FACS	SMARTseq2	750k	15'000	2'500	15	2'453	40
Wang	Kaestner	3	2	Fluidigm C1	SMARTseq2	2'200k	400'000	2'500	15	1'411	11
Xin	Gromada	12	6	Fluidigm C1	SMARTseq2	950k	350'000	4'500	15	1'371	12

Supplemental table 1: Details regarding the original datasets

Dataset	Health	Sex	Age	BMI
Baron	NDM	M	20-30	21.5
Baron	NDM	F	50-60	21.1
Baron	NDM	M	30-40	27.5
Baron	T2DM	F	50-60	29.9
Enge	NDM	M	20-30	28.4
Enge	NDM	M	20-30	24.8
Enge	NDM	F	30-40	29.5
Enge	NDM	F	40-50	23.8
Enge	NDM	M	50-60	27.3
Fang	NDM	M	20-30	20.6
Fang	NDM	M	20-30	22.8
Fang	NDM	F	30-40	34.4
Fang	NDM	M	50-60	22.0
Fang	NDM	M	20-30	30.8
Fang	NDM	M	40-50	34.6
Fang	T2DM	M	50-60	39.3
Fang	T2DM	M	60-70	28.1
Fang	T2DM	M	50-60	35.6
Lawlor	NDM	M	20-30	33.0
Lawlor	T2DM	M	50-60	35.8
Lawlor	NDM	F	50-60	22.0
Lawlor	NDM	M	20-30	23.0
Lawlor	NDM	M	30-40	55.0
Lawlor	NDM	F	50-60	26.6
Lawlor	T2DM	F	50-60	29.8
Lawlor	T2DM	F	40-50	43.0
Muraro	NDM	M	50-60	26.0
Muraro	NDM	M	20-30	22.0
Muraro	NDM	F	40-50	26.0
Muraro	NDM	M	50-60	25.0
Segerstolpe	NDM	M	40-50	30.8
Segerstolpe	NDM	M	20-30	24.7
Segerstolpe	NDM	M	20-30	21.5
Segerstolpe	NDM	F	40-50	35.0
Segerstolpe	NDM	M	20-30	32.9
Segerstolpe	NDM	M	20-30	31.8
Segerstolpe	T2DM	M	50-60	24.0
Segerstolpe	T2DM	F	30-40	39.6
Segerstolpe	T2DM	M	50-60	34.4
Segerstolpe	T2DM	F	50-60	29.8
van Gulp	NDM	M	40-50	38.8
van Gulp	NDM	M	50-60	32.6
van Gulp	NDM	M	50-60	31.8
van Gulp	NDM	F	10-20	32.4
van Gulp	NDM	M	20-30	24.8
Wang	NDM	M	50-60	29.1
Wang	T2DM	M	50-60	24.0
Wang	T2DM	F	30-40	39.3
Wang	NDM	M	20-30	39.0
Wang	NDM	F	30-40	45.2
Xin	NDM	M	20-30	21.0
Xin	NDM	F	30-40	19.0
Xin	NDM	F	20-30	24.5
Xin	NDM	F	50-60	24.1
Xin	NDM	M	20-30	31.8
Xin	NDM	M	60-70	26.0
Xin	NDM	M	20-30	23.4
Xin	NDM	M	60-70	27.3
Xin	NDM	F	20-30	25.4
Xin	NDM	M	40-50	31.7
Xin	NDM	F	30-40	28.0
Xin	NDM	M	50-60	22.8
Xin	T2DM	M	50-60	24.0
Xin	T2DM	F	30-40	39.6
Xin	T2DM	F	50-60	29.9
Xin	T2DM	F	40-50	43.1
Xin	T2DM	M	40-50	43.7
Xin	T2DM	M	50-60	24.4
Xin2	NDM	F	30-40	24.9
Xin2	NDM	M	20-30	24.8
Xin2	NDM	M	50-60	30.0
Xin2	NDM	M	50-60	22.0
Xin2	NDM	M	40-50	26.5
Xin2	NDM	F	30-40	22.9
Xin2	NDM	M	30-40	23.6
Xin2	NDM	M	20-30	30.8
Xin2	NDM	M	40-50	26.2
Xin2	NDM	F	50-60	23.5
Xin2	NDM	F	40-50	23.0
Xin2	NDM	M	50-60	21.2

Supplemental table 2: Donor specific information for all datasets used in this study

	# cells initial	Doublet removal			# Singlets		non-diabetic #					type 2 diabetic #				
		DF	Scr	both	total	islet	α	β	γ	δ	ϵ	α	β	γ	δ	ϵ
Baron	9'005	329	123	11	8'542	5'766	1'974	1'814	163	449	10	434	659	89	172	2
Enge	1'408	42	34	4	1'328	970	730	200	10	25	5	-	-	-	-	-
Lawlor	560	14	4	5	537	484	138	134	10	8	1	95	90	5	3	0
Muraro	2'116	38	17	40	2'021	1'439	847	313	99	177	3	-	-	-	-	-
Segerstolpe	2'166	63	33	14	2'056	1'459	510	147	68	55	5	431	71	122	49	1
Wang	284	4	7	5	268	262	73	40	3	4	0	96	31	11	4	0
Xin	1'503	40	1	6	1'456	1'422	341	174	24	25	0	524	271	42	21	0
							non-diabetic %					type 2 diabetic %				
							α	β	γ	δ	ϵ	α	β	γ	δ	ϵ
						Baron	44.8	41.1	3.7	10.2	0.2	32.0	48.6	6.6	12.7	0.1
						Enge	75.3	20.6	1.0	2.6	0.5					
						Lawlor	47.4	46.0	3.4	2.7	0.3	49.2	46.6	2.6	1.6	0.0
						Muraro	58.9	21.8	6.9	12.3	0.2					
						Segerstolpe	65.0	18.7	8.7	7.0	0.6	63.9	10.5	18.1	7.3	0.1
						Wang	60.8	33.3	2.5	3.3	0.0	67.6	21.8	7.7	2.8	0.0
						Xin	60.5	30.9	4.3	4.4	0.0	61.1	31.6	4.9	2.4	0.0
						Average	58.9	30.4	4.4	6.1	0.3	54.8	31.8	8.0	5.4	0.1
						SD	10.3	10.6	2.6	3.9	0.2	14.5	16.2	6.0	4.7	0.1

Supplemental table 3: The numbers and percentages of cells in each public dataset used in this study

cell-type	gene	cell-type specific function	cell-type	specificity to cell-type	pmid	pmid	pmid
alpha cells	GCG	secreted to raise blood glucose levels, paracrine signalling		glucagon is uniquely expressed in alpha cells in the pancreatic islets	25850661	27044683	15437813
alpha cells	TTR	regulates glucagon expression, more TTR expressing cells in TZD		alpha cell specific under non-diabetic conditions	this manuscript	23108050	18825272
alpha cells	HIGD1A	involved in alpha cell specific gene expression, critical for IPS alpha cell development		co-localizes with glucagon expression in adult islets	17032746	32382023	
alpha cells	SLK1A	may protect cells from oxidative stress		Expressed in alpha cells, but not beta cells	16815968	31089410	
alpha cells	GLS	produces glutamate, which enhances glucagon secretion		mainly present in alpha cells	this manuscript	15089745	26740469
alpha cells	TM4SF4	inhibits alpha and beta cell fate acquisition during development		allows FACS based enrichment for adult human alpha cells	27693023	21750032	
alpha cells	FAP	serine protease involved in paracrine signalling		co-expresses with DPP4 and GCG	25361590		
alpha cells	SLC7A2	involved in alpha cell proliferation and glucagon secretion		more highly expressed than in beta cells	https://doi.org/10.2337/db19-198-OR	33719063	
alpha cells	PCSK2	-		alpha cell specific in gene transcription and chromatin accessibility	3120862		
alpha cells	CLU	involved in glucagon processing		in humans PCSK2 is specific for alpha cells	32291281		
alpha cells	SPINT2	immunoprotective, may impact paracrine beta cell proliferation		coexpression with glucagon, alpha cell ultrastructure	10396021	11793021	
alpha cells	SERPINA1	-		smFISH stronger expression in alpha- than beta-cells	this manuscript		
alpha cells	ARX	ARX required for alpha cell development, required for ID maintenance		smFISH stronger expression in alpha- than beta-cells	this manuscript		
beta cells	INS	secreted to lower blood glucose levels, paracrine signalling		strong expression colocalization in alpha- and gamma-cells IHC	this manuscript	14561778	23785486
beta cells	IAPP	cosecreted with insulin, slows gastric emptying and promotes satiety		insulin is uniquely expressed in beta cells in the pancreatic islets	19871205	14365544	7019246
beta cells	G6PC2	beta cell specific KO shows involvement in fasting blood glucose		IHC costaining with INS, GCG, PPY and SST shows b-cell specificity	this manuscript	3276206	10341286
beta cells	ADCYAP1	provides protection against beta cell death, may be involved in proliferation		Coexpresses with insulin, not glucagon IHC	32213654	12861077	
beta cells	ERO1B	involved in insulin protein folding		strong coexpression with both insulin and glucagon IHC	12716746	12686458	
beta cells	DLK1	together with MEG3 involved in cytokine-mediated sensitivity to oxidative stress		colocalization between insulin and ERO1B in IHC	20308425	21540283	
beta cells	NPTX2	-		FACS shows beta cells can be distinguished as DLK1 high and low	30084829	24049066	
beta cells	GSN	protects beta cells from apoptosis, involved in insulin secretion		colocalization with INS, not with GCG in IHC	https://doi.org/10.32473/ufur.v21i2.108732	17192468	
beta cells	INS-IGF2	-		smFISH stronger expression in alpha- than beta-cells	26220792		
beta cells	HADH	hyperinsulinism in beta cell specific Hadh-KO mice		specifically co-expressed with insulin in b-cells	26953163	https://doi.org/10.2337/db18-1824-P	
beta cells	IGF2	involved in beta cell mass and function maintenance during stress		specifically colocalizes with INS in beta cell grafts IHC	26384384		
beta cells	PEBP1	inhibits beta cell proliferation		-	15349122		
beta cells	PFKFB2	PFKFB2 expression correlates with insulin secretion		RKIP colocalizes with beta and gamma cells in IHC	25662186		
beta cells	SLC30A8	required for in vivo insulin release		ZNT8 colocalizes with INS not GCG in human sections	19542200	28550109	
beta cells	ABCC8	encodes SUR1 critical component of Ca2+ channel, deletion leads to ID loss		-	16416420	29910119	
beta cells	SCGN	involved in beta cell specification during development,		protein expressed in alpha and beta cells IHC	782992	29702679	
gamma cells	PPY	decreases appetite, promotes satiety		localization of PPY in pancreatic islets, distinct from A-, B- and D-cells	15068960		
gamma cells	PAX6	paracrine inhibition of alpha- and beta-cell secretion of GC and INS		expressed in all islet cell-types. Colocalization with PP in IHC	9163426	10704887	
delta cells	SST	critical player in driving and maintaining delta cell identity		strong expression colocalization in alpha- and gamma-cells	this manuscript	26319183	
delta cells	LEPR	-		secreted hormone that in the pancreas is uniquely produced by delta cells	1355587		
delta cells	HHEX	paracrine inhibition of alpha- and beta-cell secretion of GC and INS		smFISH on human oct embedded pancreas shows colocalization with SST	27864352		
delta cells	CD9	-		HHEX colocalizes with SST, not with INS and GCG in IHC	24736842		
delta cells	PCSK1	-		allows enrichment for delta cells during FACS icw 2B4 and 2D12 antibodies	this manuscript		
delta cells	FFAR4	regulates somatostatin secretion		PCSK1 is upregulated and colocalizes with SST in ARX-KO hESC derived endocrine cells	26633894		
				strong colocalization of Ffar4 with Sst in mice IHC	24663807		

Supplemental table 4: literature based validation of identity genes

	total cells	α	%	β	%	γ	%	δ	%	ε	%	BH	%	other	%
Donor 1	7'788	1'880	24.1	1'225	15.7	1'786	22.9	698	9.0	48	0.6	139	1.8	2'012	25.8
Donor 2	6'764	521	7.7	1'167	17.3	2'096	31.0	1'454	21.5	610	9.0	228	3.4	688	10.2
Donor3	935	91	9.7	375	40.1	200	21.4	163	17.4	8	0.9	38	4.1	60	6.4
	15'487	2'492	16.1	2'767	17.9	4'082	26.4	2'315	14.9	666	4.3	405	2.6	2'760	17.8
α = alpha cells															
β = beta cells															
γ = gamma cells															
δ = delta cells															
ε = epsilon cells															
BH = bihormonal cells															

Supplemental table 5: Cell numbers and percentages for the gamma/delta/epsilon cell enriched dataset presented in this study

	duct -> neurog3	neurog3 -> fev	fev -> alpha	fev -> beta
α -ID			2.22	
β -ID				1.85
γ -ID				
δ -ID				
Lawlor α			2.20	
Lawlor β	-1.66			1.75
Lawlor γ				
Lawlor δ				
Muraro α	1.57	2.55	1.52	
Muraro β	-1.53	1.81		
Muraro γ	1.82	2.02		-1.70
Muraro δ	1.42	2.18		
Segerstolpe α	1.43	1.89	1.54	
Segerstolpe β		1.76		1.54
Segerstolpe γ	1.77	2.11		
Segerstolpe δ	1.53	1.92		
Xin α			1.98	
Xin β				
Xin γ				
Xin δ				

Supplemental table 6: enrichment scores for pancreas development comparing our identity genesets to genesets derived from the original studies